

Lecture Notes in Civil Engineering

Alper Ilki
Derya Çavunt
Yavuz Selim Çavunt
Editors

Building for the Future: Durable, Sustainable, Resilient

Proceedings of the
fib Symposium 2023 – Volume 2



Series Editors

Marco di Prisco, *Politecnico di Milano, Milano, Italy*

Sheng-Hong Chen, *School of Water Resources and Hydropower Engineering, Wuhan University, Wuhan, China*

Ioannis Vayas, *Institute of Steel Structures, National Technical University of Athens, Athens, Greece*

Sanjay Kumar Shukla, *School of Engineering, Edith Cowan University, Joondalup, WA, Australia*

Anuj Sharma, *Iowa State University, Ames, IA, USA*

Nagesh Kumar, *Department of Civil Engineering, Indian Institute of Science Bangalore, Bengaluru, Karnataka, India*

Chien Ming Wang, *School of Civil Engineering, The University of Queensland, Brisbane, QLD, Australia*

Lecture Notes in Civil Engineering (LNCE) publishes the latest developments in Civil Engineering—quickly, informally and in top quality. Though original research reported in proceedings and post-proceedings represents the core of LNCE, edited volumes of exceptionally high quality and interest may also be considered for publication. Volumes published in LNCE embrace all aspects and subfields of, as well as new challenges in, Civil Engineering. Topics in the series include:

- Construction and Structural Mechanics
- Building Materials
- Concrete, Steel and Timber Structures
- Geotechnical Engineering
- Earthquake Engineering
- Coastal Engineering
- Ocean and Offshore Engineering; Ships and Floating Structures
- Hydraulics, Hydrology and Water Resources Engineering
- Environmental Engineering and Sustainability
- Structural Health and Monitoring
- Surveying and Geographical Information Systems
- Indoor Environments
- Transportation and Traffic
- Risk Analysis
- Safety and Security

To submit a proposal or request further information, please contact the appropriate Springer Editor: - Pierpaolo Riva at pierpaolo.riva@springer.com (Europe and Americas);- Swati Meherishi at swati.meherishi@springer.com (Asia—except China, Australia, and New Zealand);- Wayne Hu at wayne.hu@springer.com (China).

All books in the series now indexed by Scopus and EI Compendex database!



Automated Recognition and Measurement Based on 3D Point Cloud for Precast Concrete Components Connection

Zhenfen Jin¹, Guyuan chen², Xiaowu Zhang², Wenkai Xiao², Yu Jiang²,
Zehao Zhuo², He Zhang², Yiqiang Xiang², and Jiangpeng Shu²(✉)

¹ The Architectural Design and Research Institute of Zhejiang University, Hangzhou, China

² College of Civil Engineering and Architecture, Zhejiang University, Hangzhou, China
jpeshu@zju.edu.cn

Abstract. The connection between precast concrete (PC) components is vital during the construction of prefabricated structures. However, PC components are usually inspected and measured by manual method, which is time-consuming, error-prone and unsuitable for large-scale components. This study developed a new approach for automated recognition and measurement of rebars, concrete, and sleeves on PC components based on 3D point clouds. Rebars, concrete planes, and the edge points of sleeve ports are recognized using a one-class classifier, a clustering algorithm, and the alpha-shape algorithm, respectively. Boundary estimation was performed to determine the dimensions and positions of the subcomponents. The proposed approach provides a new method for automatically recognizing rebars, concrete, and sleeves of PC components. Furthermore, the approach has the potential for PC component quality control and construction cost reduction.

Keywords: 3D Point Cloud · Automated Measurement · Automated Recognition · Connection · Precast Concrete (PC) Component

1 Introduction

Precast concrete (PC) components are widely used in prefabricated buildings and infrastructure. The performance of prefabricated structures relies heavily on the quality of PC components and their connections. Due to dimensional mismatches of rebars and sleeves of PC components during assembly, the use of PC components could suffer from connection failures and, cause severe structural destruction. As adjacent PC components are connected by rebars and sleeves and grout is poured into the sleeves to ensure the integrity of the connection, the positions of rebars and sleeves must be located precisely according to blueprints.

Quality assessment is mainly conducted manually using traditional inspection methods at present, which has limitations. First, the traditional method is time-consuming and unsuitable for large-scale components. Second, manual inspection is prone to error. To obtain a faster and more accurate approach for the connection quality control of PC

components, a 3D laser-scanning technique is used to obtain the visual information of PC components. Then, the visual information is transferred to the point clouds of PC components for further processing. By this technology, an approach was developed using algorithms for automated recognition and measurement of rebars, concrete, and sleeves of PC components based on the 3D point cloud acquired by a 3D laser scanner.

2 Methodology

First, raw data of the PC components are acquired by a 3D laser scanner. Then, the raw data are preprocessed by denoising and down sampling based on point density. After the data preprocessing is completed, the remainder is used for the recognition of the rebar, concrete, and sleeve. Next, boundary estimation is performed to determine the boundaries of the sleeve ports, concrete planes, and rebar cross-sections. At the last step, position and dimension estimation of the subcomponents are conducted. The details of each step are presented in the following sections.

2.1 Data Processing

Denoising: Considering the influence of scanning angle, scanning distance, surface material of the inspected object, and environmental factors, the acquired 3D point cloud model may contain noise [1]. It is necessary to remove as much noise as possible in the data preprocessing step. In this study, the k -nearest neighbors (KNN) algorithm [2] was used to decrease the amount of noise. The input consists of the k closest training examples in a data set. An object will be assigned to the class most common among its k nearest neighbors when using this algorithm for classification. Using KNN to denoise a point cloud, if the average distance from a point to its k -nearest neighbors is larger than a threshold value, the point is considered to be noise. In addition, a K -dimensional (KD)-tree is used to accelerate the process of searching for the nearest neighbors. Some types of 3D laser scanners contain spatial coordinates and color information, which can also be used to improve the denoising effect by the KNN algorithm if necessary [3].

Density-Based Down Sampling: The 3D point cloud needs to be down sampled given that the data are too large for calculation. In this study, a density-based down sampling algorithm was developed to reduce the point density of the overall data and retain the relative data integrity of low-density subcomponents at the same time. In the first step, the point cloud is divided into multiple grids, the amount of points in the x -, y -, and z -directions is customized. Then, every grid is assigned an index, and the points in a grid have the same index. Next, for grids that the number of points is greater than a self-defined value, the point density is calculated. After that, the down sampling ratio parameter s in every grid is calculated based on the density ratio ρ/ρ_m (ρ is the point density, ρ_m is the mean of the point density) and a benchmark value b that is customized (Eq. (1)). The number of points divided in a grid by s is equal to the number of points after being down sampled in the grid. The density ratio ρ/ρ_m is greater than 0 and the benchmark value b is set greater than or equal to 1. That means the value of s is greater than 1. Thus, the number of points in a grid will be less after being down sampled, and

the absolute difference of points in a grid between down sampling and before increases as s (or b) increases.

$$s = \frac{\rho_m}{\rho} + b \quad (1)$$

- s = down sampling ratio parameter
- ρ = point density
- ρ_m = mean of point density
- b = benchmark value

2.2 Rebar, Concrete, and Sleeve Recognition

Rebar Recognition: The major work discussed in this section is to extract points associated with rebars from the point cloud model of the component. As the rebars are not in the concrete plane and there may be a significant amount of external interference in the point cloud, the features of rebars that are different from other parts are extracted to distinguish the rebars. The one-class support vector machine (OC-SVM) algorithm [4] is used to identify points of the rebar class based on the geometric and color features of a training set of rebars. The OC-SVM algorithm maps the points of the expected class to a region where the value of the function is nonzero, while the remaining points are mapped to the origin [5]. The geometric and color features used in the OC-SVM algorithm are calculated as follows. It is assumed that there are n points in the point cloud. For every point pi ($0 < i \leq n$), in the first step, its neighbors are searched within a certain radius $rk d$ using a KD-tree. The radius $rk d$ should be greater than the diameter of the rebars. In addition, $rk d$ should not be set too large. Otherwise, the neighbors of a point located at the root of rebar will contain some points of concrete. If that occurs, the geometric features of clusters that contain a point of rebar root and its neighbors will be blurred, which may influence the accuracy of segmentation. Then, the average value of these neighbors, pm , and the differences between the neighbors and pm are calculated. The differences are encapsulated into a matrix A . Next, the covariance matrix Cov of A and the eigenvalues ($\lambda_1 \geq \lambda_2 \geq \lambda_3 \geq 0$) of Cov are calculated. Finally, the values of linearity $L\lambda$ and planarity $P\lambda$ are calculated using Eqs. (2) and (3), respectively, to characterize the geometric features of the rebars and the difference between rebars and other parts of the PC component [6]. Furthermore, red–green–blue (RGB) values are adopted as the color features of each point. Eventually, five features are used in the OC-SVM algorithm: linearity $L\lambda$, planarity $P\lambda$, R (red), G (green), and B (blue).

$$L\lambda = \frac{\lambda_1 - \lambda_2}{\lambda_1} \quad (2)$$

$$P\lambda = \frac{\lambda_2 - \lambda_3}{\lambda_1} \quad (3)$$

- $L\lambda$ = linearity
- $P\lambda$ = planarity

- $\lambda_1, \lambda_2, \lambda_3 = \text{eigenvalues of } \mathbf{Cov} (\lambda_1 \geq \lambda_2 \geq \lambda_3 \geq 0)$

Concrete Part Recognition: The density-based spatial clustering of applications with noise (DBSCAN) algorithm [7] is used to separate different concrete planes. The DBSCAN algorithm is a data clustering method used to find arbitrary shape clusters in the presence of noise.

Sleeve Recognition: In the point cloud of the component with sleeves, sleeves are usually buried inside the concrete, and their ports are on the surface of the concrete. Therefore, the main objective in this section is to recognize sleeve ports. The alpha-shape algorithm [8] is employed to extract the edge points of the sleeve ports. In computational geometry, the alpha-shape is a concept associated with the convex hull. The algorithm is based on the Delaunay triangulation of the point set. Delaunay triangulation aims to form disjoint triangular grids for points in a point cloud. The vertices of each triangular grid are the three closest points, and there is no other point in the grid.

2.3 Boundary Estimation

Boundary Estimation of Rebar Cross-Section and Sleeve Port: The edge points of the hollow square point set are estimated using the alpha-shape algorithm, as presented in Fig. 1a. The edge points are used to evaluate the performance of the algorithms by fitting the inner circle boundary, estimating the corner points, and fitting the outer square boundary. Given that the detected edge points of circle-shaped boundaries are usually not on a circle, and not evenly distributed, circle centers cannot be estimated simply by calculating the mean value of the edge points. It is necessary to fit a circle that passes closest to all the edge points on a circle-shaped boundary. A least-squares circle fitting algorithm [9] was developed to fit the inner circle boundary of the point set based on its edge points, as presented in Fig. 1a. The algorithm is a regression analysis approach to search for the best function matching the data and minimize the sum of the squared errors. The circle fitting result is shown in Fig. 1b.

Boundary Estimation of Concrete Plane: To fit the square boundary of the point set based on its edge points in Fig. 1a, a new algorithm was developed to estimate its corner points. Due to the sharp change in the geometric characteristic at the square corners, the curvature change value C_λ [6] for every edge point on the square boundary is calculated to quantify the degree of change. It is assumed that there are n points on the square boundary. The curvature change value of a point p_i ($0 < i \leq n$) is calculated as follows. First, for every point p_i , its neighbors within a certain radius r_{kd} are searched. Then, the average value of these neighbors, p_m , and the differences between the neighbors and p_m are calculated. The differences are encapsulated into a matrix A . Next, the covariance matrix \mathbf{Cov} of A and the eigenvalues ($\lambda_1 \geq \lambda_2 \geq \lambda_3 \geq 0$) of \mathbf{Cov} are calculated. Finally, the geometric feature (i.e., curvature change value C_λ), is calculated as Eq. (4) to quantify the geometric change of the square boundary.

$$C_\lambda = \frac{\lambda_3}{\lambda_1 + \lambda_2 + \lambda_3} \quad (4)$$

- $C_\lambda = \text{curvature change value}$

- $\lambda_1, \lambda_2, \lambda_3 = \text{eigenvalues of } \mathbf{Cov}$

By calculating the $C\lambda$ of every concrete edge point, the points on the corners are detected according to the larger values of $C\lambda$. After applying the DBSCAN algorithm on the corner points and separating them into four parts, four initial corner points are created by calculating the average value of points in every part. Then, points within a certain width between the two adjacent initial corner points are separated as the points of a square sideline. Given the geometric features of the square boundary, the side-lines of the square are straight. Therefore, the least-squares line fitting algorithm is used to fit every sideline. Finally, four true concrete corner points are estimated by solving a system of linear equations in two unknowns of every two adjacent sidelines, as shown in Fig. 1b.

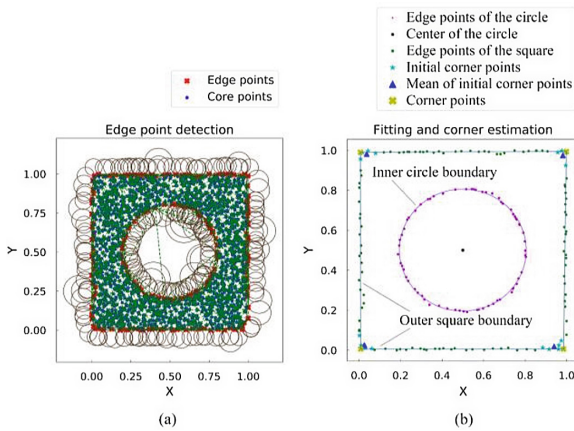


Fig. 1. (a) Edge point detection result of a hollow square point set ($\alpha = 2$) and (b) location of the inner circle boundary and outer square boundary.

2.4 Position and Dimension Estimation

In the point cloud model of the component with rebars, rebars are first recognized and segmented from the point cloud. Then, the concrete part is processed by the concrete part recognition approach to separate different concrete planes, which are divided into the concrete plane where rebars are located and other planes. Next, the former concrete plane is projected onto the 2D plane, which is parallel to the concrete plane. The edge points of the outer square boundary of the rebar-located concrete plane are extracted using the alpha-shape algorithm. Furthermore, rebar-associated points are projected onto the 2D plane. Eventually, the corner points of the concrete plane are estimated, and the sidelines of the concrete plane are fitted by using the least-squares line fitting algorithm.

In the point cloud model of the component with sleeves, the first step is to separate the concrete plane with sleeve ports from other planes after segmenting different concrete planes. Then, after projecting the concrete plane to the 2D plane which is parallel to the concrete plane, the edge points of the sleeve ports and the outer square boundary of the concrete plane are extracted using the alpha-shape algorithm. Eventually, the corner points of the concrete plane are estimated, and the sidelines of the concrete plane and the inner circle boundaries of the sleeve ports are fitted by the least-squares fitting algorithm. The positions of the rebars and sleeves can be estimated by calculating the distances between adjacent rebars or sleeve centers and those from the centers to their nearest concrete boundary. To calculate the length of rebars, the principal component analysis (PCA) algorithm is employed. Using the PCA algorithm, the maximum covariance value of the points that are associated with rebar is calculated to determine the vector direction of the rebar central axis. Then, the rebar length can be calculated based on the vector direction.

3 Experiments and Validation

3.1 Validation Experiments

Two PC components were cast to validate the effectiveness of the developed automated recognition and measurement approach (see Fig. 2). The components are two parts of a column, which can be assembled by connecting the rebars and sleeves. The dimensions of the PC component with rebars are 400 mm (length) \times 400 mm (width) \times 600 mm (height), and eight rebars were located at the top of the component, with an average spacing of approximately 148 mm. The one with sleeves had the same size of dimensions to that with rebars, and eight sleeves were buried in the concrete, with the same average spacing to that of the rebars (see Fig. 2b). The two PC components were scanned by a 3D laser scanner, and their dimensions and positions were estimated using the developed approach. The manual point cloud segmentation was conducted the open-source 3D point cloud mesh processing software CloudCompare [10]. All coding was completed in the PyCharm IDE [11], using Python programming language.

In this study, a terrestrial laser scanner (TLS) of the FARO Focus series (Focuss 350) [12] was used to acquire 3D point clouds. In the process of scanning PC components, the position of the scanner was located approximately 1.5 m from the PC components, and the position was changed two times to obtain the visual information of all sides and the top of the PC components. The acquired point clouds are plotted in Fig. 3.

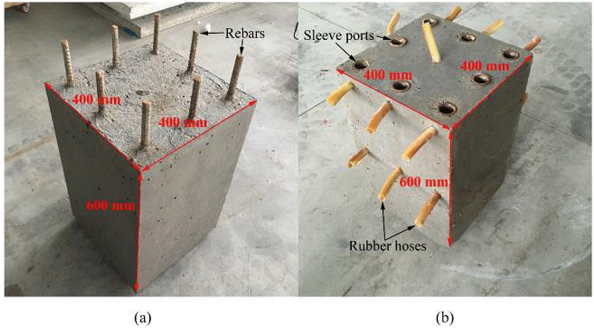


Fig. 2. Validation column specimens: the PC component with (a) sleeves and (b) rebars.

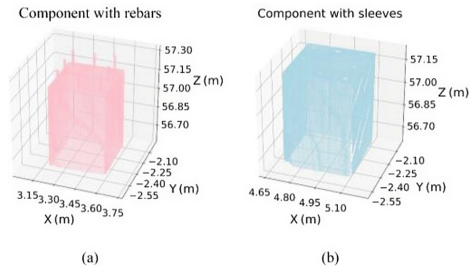


Fig. 3. Point cloud model of the PC component with (a) sleeves and (b) rebars.

3.2 Experimental Results

After preprocessing the point cloud model of the two PC components, recognition tasks were conducted to separate different subcomponents. For the point cloud model of the PC component with rebars, the OC-SVM algorithm was first used to extract points associated with rebars. The obtained points did not indicate all the data of rebars but only some of them because of the sensitivity of the parameter settings. However, this can be revised in the subsequent steps. By extracting smaller dense areas in the Gaussian sphere space in the process of concrete plane recognition, more points were determined as initial noise, which contained massive points associated with rebars (see Fig. 4). After the concrete part recognition, the initial noise was classified into their closest class by the modified KNN algorithm.

The procedure of the proposed recognition approach used on the point cloud model of the PC component with rebars is shown in Fig. 5. In procedure I, the point cloud model (see Fig. 5a) is segmented into separated rebars (see Fig. 5b) and the concrete part (see Fig. 5c) through rebar recognition. In procedure II, the concrete part is segmented into separated concrete planes by concrete recognition (see Fig. 5d). In procedure III, the concrete plane where rebars are located is selected for edge point detection (see Fig. 5e). Combining the edge points of the outer boundary of the concrete plane and rebars, the measurement task was performed based on all edge points in Fig. 5f.

For the point cloud model of the PC component with sleeves, the procedure of the proposed recognition approach is shown in Fig. 6. In procedure I, concrete recognition was conducted based on the point cloud model (see Fig. 6a) to separate different concrete

planes (see Fig. 6b). In procedure II, the concrete plane with sleeve ports was selected and reduced to a 2D plane. Sleeves were recognized by detecting the edge points of the sleeve ports using the alpha-shape algorithm (see Fig. 6c). The measurement task was performed based on the edge points in Fig. 6d.

After the edge points were obtained, the proposed corner estimation approach was employed to estimate the corners of the concrete boundary. In the process of estimating the concrete corner points, the threshold of curvature change $C\lambda$ was set to the highest score of $C\lambda$ (excluding outliers) because the values of $C\lambda$ surged at concrete corners. The least-squares line fitting algorithm was used to fit the sidelines of the concrete planes. In addition, the least-squares circle fitting algorithm was used to fit the boundaries of the rebar cross-sections and the inner boundaries of the sleeve ports. Considering that the points on the top and root of the rebars influenced the accuracy of circle fitting, the middle sections of rebars were selected to fit the boundaries of the rebar cross-sections. Fig. 7 shows the results of the corner estimation and line fitting of the concrete boundaries as well as the circle fitting of the rebar cross-sections and sleeve ports. The results show that the developed automated approach can identify and locate the positions of subcomponents effectively.

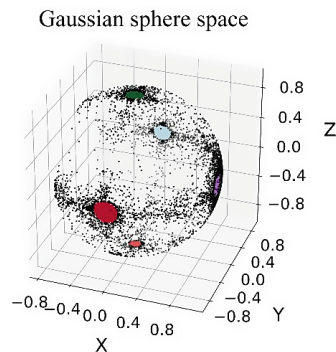


Fig. 4. Points in the point cloud mapping to a Gaussian sphere using their normal vectors, and clusters identified using the DBSCAN algorithm.

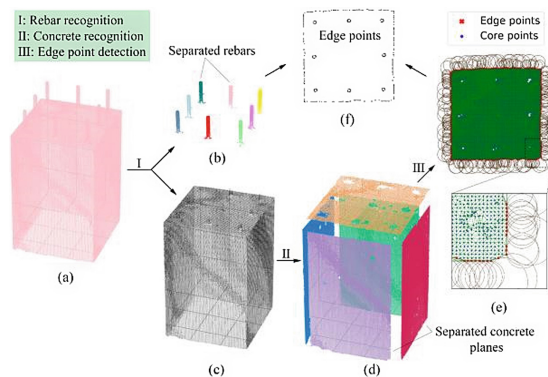


Fig. 5. Procedure of the proposed recognition approach used on the point cloud model of the PC component with rebars.

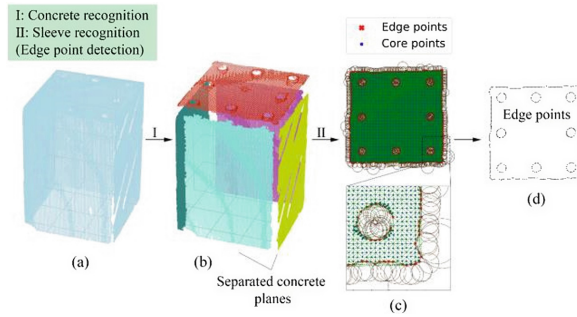


Fig. 6. Procedure of the proposed recognition approach used on the point cloud model of the PC component with sleeves.

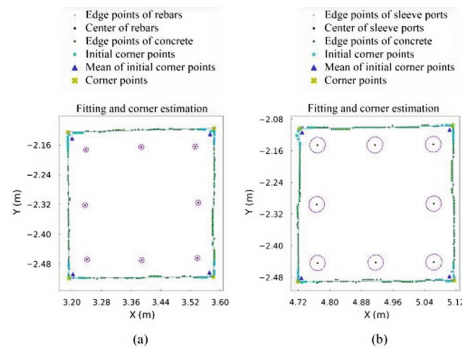


Fig. 7. Recognition and position estimation of (a) rebars and (b) sleeves.

4 Conclusions

A new approach was developed with for automated recognition and measurement of PC components as well as rebars and sleeves, based on the 3D point cloud acquired using a 3D laser scanner. A density-based down sampling algorithm is developed that can retain the data integrity of rebars. Rebars can be recognized successfully using the one-class support vector machine (OC-SVM) algorithm. The concrete planes with rebars or sleeve ports were recognized accurately by the plane recognition approach. The edge points on the inner boundaries of the sleeve ports were estimated using the alpha-shape algorithm based on the Delaunay triangulation result. The corner points and sidelines of the concrete planes (where rebars or sleeve ports were located) were estimated using the corner point estimation approach and the least-squares line fitting algorithm, respectively. The results indicate that the developed approach can recognize rebars and sleeves and estimate their accurate positions automatically.

Acknowledgements. The authors gratefully acknowledge the financial supports by the Key R&D Program of Zhejiang (2023C01161). In addition, the author Chenhang Sheng has contributed to our research and we would like to add his name into the paper, after the names of other authors.

References

1. Hebert M, Krotkov E (1992) 3D measurements from imaging laser radars: how good are they? *Image Vis Comput* 10:170–178
2. Peterson L (2009) K-nearest neighbor. *Scholarpedia* 4:2009
3. Wang Q, Cheng JCP, Sohn H (2017) Automated estimation of reinforced precast concrete rebar positions using colored laser scan data. *Comput-Aided Civil Infrastruct Eng* 32:787–802
4. Mazhelis O (2006) One-class classifiers: a review and analysis of suitability in the context of mobile-masquerader detection. *South Afr Comput J*, 29–48
5. Schölkopf B, Platt JC, Shawe-Taylor J, Smola AJ, Williamson RC (2001) Estimating the support of a high-dimensional distribution. *Neural Comput* (13):1443–1471
6. Blomley R, Weinmann M, Leitloff J, Jutzi B (2014) Shape distribution features for point cloud analysis – a geometric histogram approach on multiple scales. *ISPRS Ann Photogram Remote Sens Spatial Inf Sci* (II-3):9–16
7. Ester M, Kriegel H-P, Sander J, Xu X (1996) A density-based algorithm for discovering clusters in large spatial databases with noise. In: *Proceedings of the 2nd International Conference on Knowledge Discovery and Data Mining*. AAAI Press, Portland Oregon
8. Kirkpatrick DG, Seidel R (1983) On the shape of a set of points in the plane. *IEEE Trans Inf Theory* 29:551–559
9. Maisonobe L (2007) Finding the circle that best fits a set of points
10. Girardeau-Montaut D (2015) CloudCompare: 3D point cloud and mesh processing software, <http://www.cloudcompare.org>
11. JetBrains (2021) PyCharm: the Python IDE for Professional Developers by JetBrains
12. Atkinson GA, Zhang W, Hansen MF, Holloway ML, Napier AA (2020) Image segmentation of underfloor scenes using a mask regions convolutional neural network with two-stage transfer learning. *Autom Constr* 113:103–118